A Model Study of Rigid Pavement Behavior Under Corner and Edge Loadings

PAUL F. CARLTON, *Chief of Research Analysis Branch*, and
RUTH M. BEHRMANN, *Research Mathematician*,
Ohio River Division Laboratories, Corps of Engineers, U. S. Army

Results of laboratory tests, using small scale models, are presented and compared with theoretical analyses of critical stresses resulting from single-wheel loads acting at a free corner and at a free edge of a rigid pavement slab.

Included are a brief description of the design and construction of the model, test procedures used, presentation of the data therefrom and its analysis. Principally, the testing involved the measurement of strains in a plaster slab subjected to static loading as follows: (1) loads tangent to a free edge and at a considerable distance from any corner; and (2) loads tangent to both edges of the slab at a free corner. By using various sizes of both circular and elliptical contact areas in loading the slab, and by expressing the stress comparisons in non-dimensional terms, relationships between critical pavement stresses for corner and edge loadings are established which are applicable to the prototype as well as to the model.

● SINCE 1940, the Corps of Engineers, through the Rigid Pavement Investigational Program conducted by the Ohio River Division Laboratories, has endeavored to develop a complete understanding of the behavior of rigid pavement under various conditions of loading. Condition surveys and performance studies have shown that approximately 90 percent of structural breaks (pavement cracks) of both airfield and highway pavements are transverse to the direction of traffic. This type of failure indicates that the most severe loading condition occurs when the load is at or near a longitudinal edge of a pavement slab. However, from the standpoint of pavement deterioration from continued traffic, corner breaks, although relatively few in number, are more detrimental than transverse cracks, and have been the object of several extensive research investigations during the past 30 years (1, 2, 3). These previous investigations far exceed the scope of the work covered by this report, which is limited to the presentation of recent findings regarding the relationship between stresses produced by corner and edge loadings. This study is unique, however, in that it was conducted in the laboratory using small scale models. Previous experience at the Ohio River Division

sion Laboratories (4) has shown that such models can be utilized with considerable success for investigating stresses resulting from various loading arrangements. The laboratory methods employed provide greater control over the several variables involved than can be obtained in field tests. Since conditions of controlled temperature and humidity were maintained during testing, warping due to temperature and moisture gradients in the slab were virtually eliminated. In addition, the physical properties of the slab and subgrade were controlled and measured more precisely in the laboratory than is possible in the field.

DESIGN OF THE MODEL

Theoretical Considerations

So that the results obtained from the model tests might be correlated with Westergaard's theoretical analyses of rigid pavement behavior, it was necessary in the design of the model that consideration be given to the simulation of certain basic assumptions inherent in these theoretical analyses. The assumptions and conditions simulated include: (1) that the subgrade be uniform in character and provide continuous support for the slab; (2) that the

relationship between the size of the loaded area and the thickness of the slab be such that the ordinary theory for the bending of thin plates is applicable; (3) that the slab be a homogeneous, isotropic material of uniform thickness; (4) that the critical stresses remain within the elastic limits of both the slab and the subgrade; (5) that the horizontal dimensions of the slab be such that the slab acts as though it were infinite in horizontal extent; (6) that the depth of the subgrade be such that it may be considered infinite; and (7) that, for corner loadings, the loaded area be symmetrical about the diagonal bisector of the corner angle.

Westergaard, in his analyses, introduced the term "radius of relative stiffness," which he denoted by l. This term reflects the relationship between the stiffness of the slab and the resistance of the subgrade to vertical displacement. In comparing theory, model, and prototype, various dimensions and relationships may b e expressed as functions of l.

Edge Loadings

The theoretical maximum stresses developed in the model slab for loadings tangent to a free edge were computed in accordance with Westergaard's Equation 12 (5) as follows:

$$\sigma_e = \frac{3(1 + \mu)P}{\pi(3 + \mu)h^2} \left[\log \frac{Eh^3}{100k \left(\dfrac{a + b}{2} \right)^4} \right.$$

$$+ 1.84 - \frac{4}{3}\mu + (1 + \mu)\frac{a - b}{a + b}$$

$$\left. + 2(1 - \mu)\frac{ab}{(a + b)^2} + 1.18(1 + 2\mu)\frac{b}{l} \right]$$

where: μ = Poisson's ratio for the slab.
E = modulus of elasticity of the slab.
h = slab thickness.
k = subgrade modulus.
P = load on the footprint.
a = semi-major axis of the footprint.
b = semi-minor axis of the footprint.
l = radius of relative stiffness of the slab and is defined as:

$$\left[\frac{Eh^3}{12(1 - \mu^2)k} \right]^{1/4}$$

For edge loading, the critical stress occurs at the bottom edge of the slab, at the point of tangency, and acts in a direction parallel to the edge.

Corner Loadings

Theoretical analysis of slab behavior at a free corner is limited largely to Westergaard's early work. In a paper in April, 1926 (6) Westergaard gave the following equation for the determination of maximum stress at the corner:

$$\sigma_c = \frac{3P}{h^2} \left[1 - \left(\frac{a\sqrt{2}}{l} \right)^{0.6} \right]$$

where: P = load on the footprint.
h = slab thickness.
a = radius of the footprint.
l = radius of relative stiffness of the slab.

For corner loadings symmetrical about the diagonal bisector of the corner angle (a condition assumed in the above equation), the critical corner stress occurs in the top of the slab along the diagonal bisector and acts in a direction parallel to the diagonal bisector.

In his April 1926 paper, Westergaard also gave the following equation for finding the distance from the corner, along the diagonal bisector of the corner angle, that the maximum stress occurs:

$$d = 2.3785 \, (al)^{1/2}$$

where a = radius of the footprint.
l = radius of relative stiffness of the slab.

Description of the Model

A general view of the model table and equipment used in these tests is shown in Figure 1. The prototype slab is simulated in the model by a 15″ x 15″ x 0.125″ Hydrostone gypsum cement slab having a modulus of elasticity, E, of 3.0 × 10⁶ pounds per square inch and a Poisson's ratio, μ, of 0.25. The subgrade is simulated by a 24″ x 24″ x 12″ block of natural rubber supported rigidly by a concrete table. Small lead cubes are distributed uniformly over the slab to insure its being in continuous contact with the rubber subgrade, a basic assumption in the Westergaard analyses, and their presence does not affect the elastic

action of the slab. Using various sizes of circular and elliptical footprints, static loads are applied to the slab by means of the reaction beam.

In addition to the physical properties of the slab, the effective modulus of subgrade reaction, k, must be known. Values of k, for both corner and edge loadings, were determined experimentally; and were based on the volumetric displacement of the subgrade within the limits of the slab. For edge loadings a static load of 7.5 pounds was applied to a 0.4-inch radius circular footprint placed tangent to an edge of the slab. For corner loading, a static load of 8.0 pounds was applied to a 0.5-inch radius circular footprint placed tangent to both edges at a corner of the slab. In these tests the choice of the footprint size and static load was arbitrary inasmuch as the load was transmitted to the subgrade by the pavement slab rather than by the footprint bearing directly on the subgrade.

Slab deflections were measured to the nearest 0.0001 inch and at 1-inch intervals longitudinally and transversely around the loaded areas. From the deflection data, contours of equal slab deflection were plotted on a scaled drawing of the slab. Assuming there was no volume change in the slab, the deflections measured represented the vertical displacement of the subgrade. The total volumetric displacement of the subgrade, within the limits of the slab, was then computed from a summation of the individual volumes determined for each deflection contour. The subgrade modulus for each type of loading
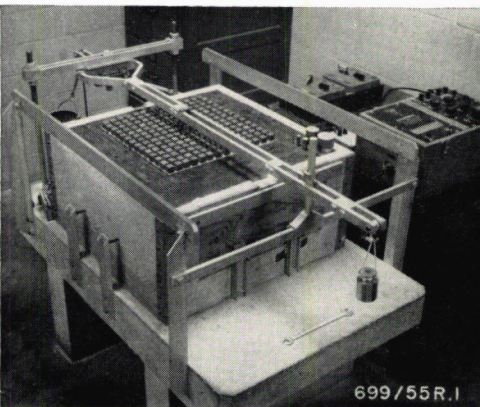

Figure 1. General view of the model table and equipment.

SUBGRADE MODULUS AT SLAB EDGE

$K = \dfrac{P}{V}$, WHERE K= SUBGRADE MODULUS, P=LOAD, AND V=VOLUME OF SUBGRADE DISPLACED
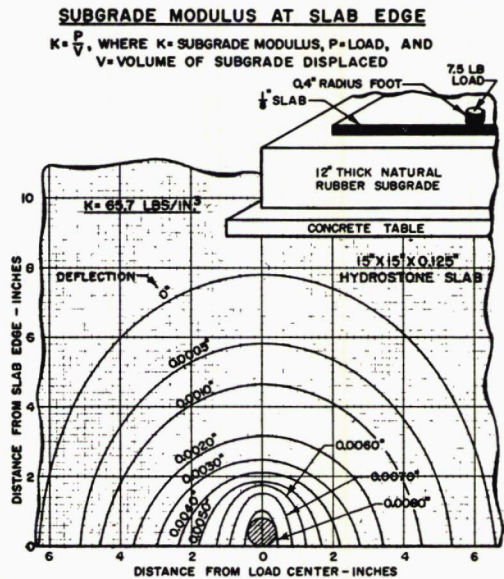
Figure 2. Loading arrangement and slab deflection contours for determination of subgrade modulus at a free edge.

was then obtained from the relationship:

$$k = P/V$$

where: P = total load applied to the footprint.

V = volumetric displacement of the subgrade.

The loading arrangements and contours of equal slab deflection, for the determination of k at a free edge and at a free corner, are shown in Figures 2 and 3, respectively. Based on these data, the effective subgrade modulus was determined to be 67.0 pounds per cubic inch for corner loadings, and 65.7 pounds per cubic inch for edge loadings. For purposes of analysis in this report, k was assumed to be 65.0 pounds per cubic inch for both corner and edge loadings.

Using the elastic constants of the model slab and subgrade, as given above, the radius of relative stiffness, l, of the model slab was approximately 1.7 inches. In terms of l, the horizontal dimensions of the slab were only slightly less than $9l$ x $9l$, which satisfied the assumption that the slab was infinite with regard to horizontal extent. Similarly, the thickness of the rubber subgrade was approximately $7l$, which satisfied the assumption

that the subgrade was, in effect, infinite in depth.

CONSTRUCTION OF THE MODEL SLAB

Using standard procedures for mixing and blending the Hydrostone cement, the test slab was cast in a steel form glued to a glass plate. Immediately after pouring, the slab was struck off with a second glass plate, this strike-off plate being left in place on top of the slab for approximately one hour. The use of glass plates to form both the top and bottom sides of the test slab insured smooth plane surfaces and a thickness uniform within plus or minus 0.002 inch. After permitting the slab to cure in air at room temperature for seven days, 23 Type A-7, SR-4 strain gages were cemented to the slab as follows: 17 gages for measuring strains at the edge, corner-edge, and on and parallel to the corner-diagonal were mounted on the underneath side of the slab; 6 gages for measuring strains perpendicular to the corner-diagonal were mounted on the top side of the slab. Figure 4 shows the orientation and spacing of the gages with respect to the corner and the edges of the slab.
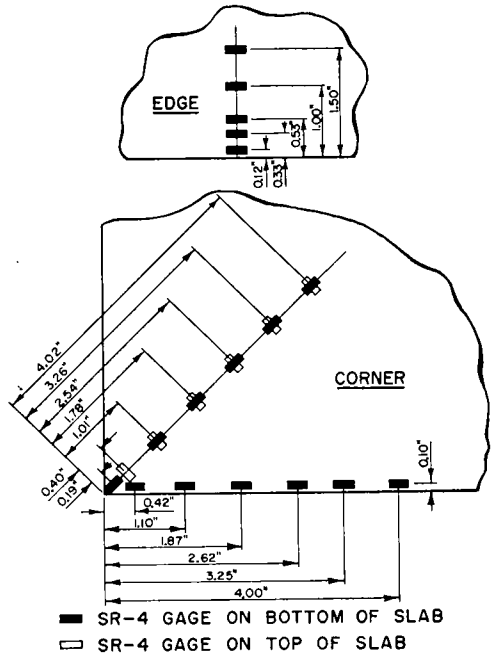

Figure 4. Orientation and spacing of SR-4 strain gages on the model slab.
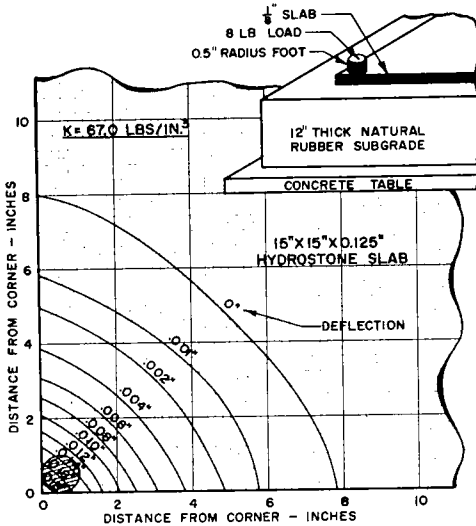

Figure 3. Loading arrangement and slab deflection contours for determination of subgrade modulus at a free corner.

TEST PROCEDURE

After allowing the strain gages to air-dry for a minimum period of 48 hours, the test slab was placed directly on the rubber subgrade. A layer of ¾-inch lead cubes was then distributed uniformly over the top surface of the slab (see Figure 1). Static loads were applied to the slab by means of the reaction beam and the various sizes of footprints as follows: circular footprints having radii of 0.1″, 0.2″, 0.3″, 0.4″, 0.5″, and 0.75″; and elliptical footprints having semi-axes of 0.15″ x 0.10″, 0.30″ x 0.19″, 0.51″ x 0.31″, 0.69″ x 0.40″, and 0.96″ x 0.60″. A static load of eight pounds was used for all footprints and both corner and edge loadings. Inasmuch as the strains in the slab are proportional to the load applied to the footprint, the choice of the test load was arbitrary and limited only by the working stresses of the Hydrostone and a reasonable factor of safety against accidental failure of the slab during testing.

For edge loadings, the footprints were placed tangent to the edge at a point approximately at the center of one edge of the slab. In this way there was sufficient distance be-

tween the point of application of the edge loadings and the adjacent corners of the slab to eliminate any effect of the corners on the edge strains. All elliptical footprints were oriented so that their major axes were parallel to the edge. (Note: Previous model tests had shown that this orientation of an elliptical footprint produces the maximum edge stress.)

For corner loadings, both the circular and the elliptical footprints were positioned tangent to the two edges at the corner. Inasmuch as strain gages were mounted on the corner diagonal and along one edge of the corner only, three different orientations of the elliptical footprints were required to investigate all possibilities of critical loading:

E_1—with the major axes parallel to and on the diagonal bisector of the corner angle.

E_2—with the major axes parallel to the corner edge on which the strain gages were mounted.

E_3—with the major axes perpendicular to the corner edge on which the strain gages were mounted.

DETERMINATION OF UNIT STRESSES

In order to analyze better the strain data obtained from the model, the maximum measured strains were converted to corresponding maximum unit stresses by means of the following equations (7):

$$E\epsilon_x = \sigma_x - \mu(\sigma_y + \sigma_z) \qquad (1)$$

$$E\epsilon_y = \sigma_y - \mu(\sigma_x + \sigma_z) \qquad (2)$$

For this study the assumption $\sigma_z = 0$ was made. Substitution of this assumption in Equations 1 and 2 results in:

$$E\epsilon_x = \sigma_x - \mu\sigma_y \qquad (3)$$

$$E\epsilon_y = \sigma_y - \mu\sigma_x \qquad (4)$$

Edge and Corner-Edge Stresses

For loading at a free edge, $\sigma_y = 0$ at the edge. The maximum edge stress, σ_x, was then determined from Equation 3 to be

$$\sigma_x = E\epsilon_x$$

where: σ_x = maximum edge stress in the direction parallel to the edge.

E = modulus of elasticity of the Hydrostone.

ϵ_x = maximum measured edge strain parallel to the edge.

Corner-Diagonal Stresses

Assuming that the maximum strain or stress lies on and parallel to the bisector of the corner angle for corner loadings, the maximum measured strains along the diagonal were converted to maximum unit stresses using Equations 3 and 4 modified as follows:

$$E\epsilon_d = \sigma_d - \mu\sigma_n \qquad (3a)$$

$$E\epsilon_n = \sigma_n - \mu\sigma_d \qquad (4a)$$

Combining Equations 3a and 4a gives the maximum stress, σ_d, at a point on the diagonal bisector of the corner angle to be

$$\sigma_d = \frac{E(\epsilon_d + \mu\epsilon_n)}{1 - \mu^2}$$

where: μ = Poisson's ratio for Hydrostone.

E = modulus of elasticity of Hydrostone.

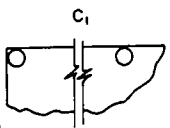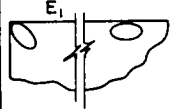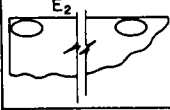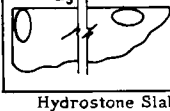ϵ_d = measured maximum strain along the diagonal bisector of the corner angle.

ϵ_n = measured strain normal to the diagonal at the point of maximum strain along the diagonal.

σ_d = measured maximum stress at a point on the diagonal bisector of the corner angle.

TEST RESULTS

The magnitude and location of the maximum strains obtained from the model slab for the circular loadings and the three cases of the elliptical loadings are shown in Table 1. The maximum strains for corner-edge and corner-diagonal loadings were determined from curves plotted from the strains indicated by the individual SR-4 gages. In the case of the edge loadings, however, the width of the strain gages precluded mounting any gage such that its effective center would be at the edge of the slab (in these tests, the center of the gage nearest the edge was 0.12 inch from the edge). It was necessary, therefore, to obtain the maximum strain at the edge of the slab by extrapolation from the strains indicated by the five gages, in line, normal to the edge. In the case of the corner-edge loadings, no extrapolation was made as it was assumed that strains at the gage position and the edge lay on the same equi-strain contour about the corner.

TABLE 1
LOCATION AND MAGNITUDE OF MAXIMUM EDGE AND CORNER STRAINS

Type of Loading	Footprint Radius or Semi-Axes, Inches	A/l^2	Edge Maximum Strain x 10^4, In./In.	Corner-Diagonal Maximum Parallel Strain x 10^4 In./In.	Corner-Diagonal Maximum Normal Strain x 10^4 In./In.	Corner-Diagonal Distance from Corner, Inches	Corner-Edge Maximum Strain x 10^4 In./In.	Corner-Edge Distance from Corner, Inches
C_1	0.10	0.0111	6.03	3.56	1.80	0.90	2.18	1.55
	0.20	0.0444	4.58	2.72	1.38	1.15	1.80	1.75
	0.30	0.0999	3.76	2.27	1.12	1.38	1.52	2.00
	0.40	0.1775	3.19	1.89	0.98	1.56	1.24	2.32
	0.50	0.2775	2.76	1.48	0.72	1.95	1.05	2.62
	0.75	0.6244	2.02	0.98	0.46	2.84	0.80	3.40
E_1	0.15 x 0.10	0.0166	5.40	3.26	1.58	0.92	2.08	1.60
	0.30 x 0.19	0.0633	4.07	2.34	1.23	1.22	1.63	1.87
	0.51 x 0.31	0.1755	3.08	1.53	0.87	1.66	1.22	2.30
	0.69 x 0.40	0.3063	2.55	1.15	0.67	2.06	0.98	2.63
	0.96 x 0.60	0.6392	1.90	0.80	0.39	2.86	0.73	3.10
E_2	0.15 x 0.10	0.0166	5.40	3.28		0.90	2.05	1.65
	0.30 x 0.19	0.0633	4.07	2.45		1.18	1.62	2.20
	0.51 x 0.31	0.1755	3.08	1.58		1.64	1.19	2.90
	0.69 x 0.40	0.3063	2.55	1.17		2.02	0.92	3.25
	0.96 x 0.60	0.6392	1.90	0.80		2.86	0.68	3.50
E_3	0.15 x 0.10	0.0166	5.40	3.28		0.90	2.12	1.58
	0.30 x 0.19	0.0633	4.07	2.45		1.18	1.79	1.82
	0.51 x 0.31	0.1755	3.08	1.58		1.64	1.32	2.17
	0.69 x 0.40	0.3063	2.55	1.17		2.02	1.07	2.44
	0.96 x 0.60	0.6392	1.90	0.80		2.86	0.77	2.85

Hydrostone Slab 15" x 15" x 0.125", $E = 3.0 \times 10^6$ lbs/in.^{2}, $\mu = 0.25$, $k = 65$ lbs/in.^{3}, $P = 8$ lbs., $l = 1.6825$ in.

The maximum strains measured in the model were converted to unit stresses as described above, and the corresponding theoretical stresses were computed from the Westergaard equations given previously. A comparison of maximum corner and edge stresses, both theoretical and observed, is shown in Figure 5. The stresses are plotted versus A/l^2, where A is the contact area of the footprint. Inasmuch as l is in the form of a linear dimension, the expression A/l^2 is non-dimensional. Thus, this method of analysis allows the direct application to the prototype of stress relationships developed in the model. The various footprint sizes used in applying the load to the slab provided a range in values of A/l^2 which includes most prototype conditions.

A percentage comparison of the maximum corner stress to the maximum edge stress for both the model and the theory is shown in Figure 6.

The distance from the corner to the point of maximum stress along the diagonal bisector of the corner angle, as determined theoretically and experimentally, are compared in Figure 7.

DISCUSSION OF TEST RESULTS AND ANALYSES

Slab Stresses

A comparison of the measured strains along the diagonal bisector of the corner angle, as given in Table 1, shows that the strains along the diagonal are practically equal for all three cases of elliptical loading E_1, E_2 and E_3. This was reasonable inasmuch as there was no change in the distance from the corner to the centroid of a given footprint for the three load positions, and only small changes were required relative to the positioning of the footprints. Therefore, it was assumed that no significant differences existed between the maximum corner stresses, for a given footprint, for the three loadings E_1, E_2 and E_3. On this basis, the unit stresses determined for the symmetrical loading E_1 were considered as representing the maximum stresses for all corner loadings using elliptical footprints. Since Westergaard's analyses of corner stresses were valid only for a circular loaded area, no theoretical stresses could be determined for comparison with the stresses measured in the

model using elliptical footprints. Also, with regard to the stresses at the corner-edge, no theoretical analysis for the determination of these stresses was available. From the comparison of corner-edge and corner-diagonal stresses, as shown in Figure 5, it is apparent that only for the smaller values of A/l^2 are the corner-edge stresses appreciably less severe than those along the corner-diagonal.

For the elliptical loadings E_2 and E_3, the measured strains along the diagonal bisector of the corner angle should have been identical for any footprint. However, due to the various sources of error such as positioning the footprints, alignment of strain gages, and accuracy of the instruments used to measure the strains, some differences in comparable strains were noted. For purposes of analysis, average values of the corner-diagonal strains for loadings E_2 and E_3 were used. It is of some significance to note that the average difference between comparable strains for the E_2 and E_3 loadings was only slightly more than 3 percent.

It can be seen from Figures 5 and 6 that the shape of the loaded area, whether circular or elliptical, has little effect on the pavement stress for a given value of A/l^2. Actually, the shape of the footprint results in less than 5 percent variation in stress. Since prototype footprint shapes are actually somewhere between being circular or elliptical, the average data obtained from the circular and elliptical loadings can be applied to the prototype with negligible error.

In general, it may be said that the agreement between the behavior of the model and that predicted by Westergaard's theoretical analyses was good. As has been noted in previous studies using similar models, the maximum edge stresses observed in the model were from 10 to 12 percent less than the theoretical stresses. In the case of the maximum corner stresses, however, the stresses measured in the model were only 65 to 75 percent as great as those determined from the Westergaard equations.

Figure 6 shows a percentage comparison of the maximum corner stress to the maximum edge stress for both the model and the theory. Again, the stress relationships are plotted versus A/l^2. It can be seen in this figure that for either the model or the theory, the ratio between maximum corner and edge stresses does not vary more than plus or minus 6 per-

cent throughout the range of values of A/l^2 tested.

Particularly good agreement, as is indicated by Figure 7, was obtained between the model
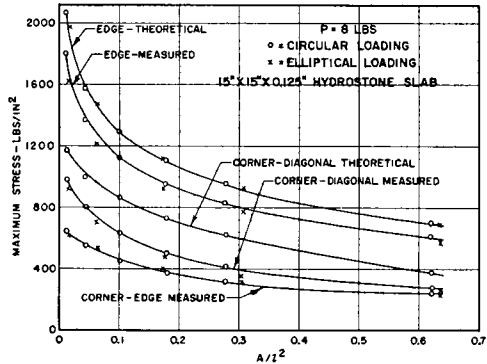

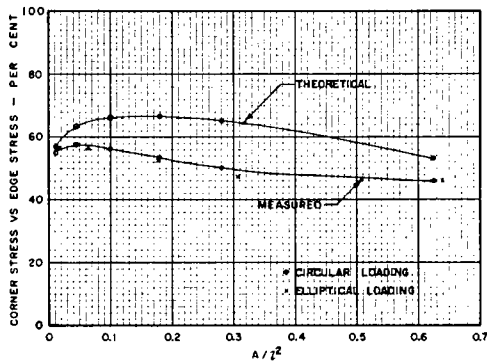Figure 5. Measured and theoretical maximum corner and edge stresses.

Figure 6. Relationship of corner stress to edge stress as observed in the model and from Westergaard's analyses.
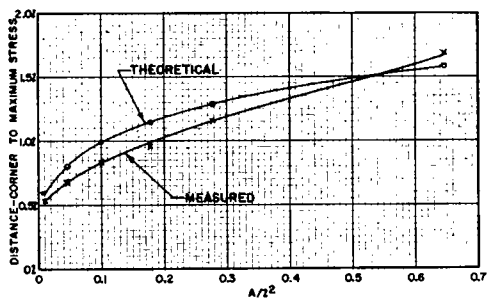

Figure 7. Location of maximum corner stress along the diagonal bisector of the corner as observed in the models and from Westergaard's analyses.

and the theory with respect to the location of the maximum stress along the corner diagonal for corner loadings.

Subgrade Modulus

From the data obtained in this study, it appears that the effective subgrade modulus is the same for both corner and edge loadings. In previous model tests, however, determinations of the subgrade modulus for the model had shown that for interior loadings, the effective k was 35 pounds per cubic inch. This is approximately half the value of k measured at the edge and at the corner. It is believed that this apparent increase in k near the boundaries of the slab may be explained by the additional support derived from the subgrade outside the limits of the slab.

CONCLUSIONS

The type of model employed in these tests is essentially an analog device and as such, may be applied to a variety of problems involving special conditions of loading of rigid pavements. The agreement between the behavior of the model and that predicted by Westergaard's theoretical analysis was generally good, especially when it is considered that the accuracy of analogs of this type is seldom better than 5 to 10 percent.

For the specific assumptions and conditions enumerated earlier, the following conclusions have been drawn:

1. The effective subgrade modulus is the same for both edge and corner loadings.

2. The maximum corner stress is not appreciably affected by the orientation of an elliptical footprint. However, for corner loadings of the elliptical footprint with axes parallel to the corner edges, maximum strains in the corner-edge parallel to the minor axes of the footprints were slightly greater than maximum strains in the corner-edge parallel to the major axes of the footprints.

3. The shape of the loaded area, whether circular or elliptical, has little effect on the pavement stress for equal values of A/l^2.

4. Maximum corner stresses in the top surface of the slab are tensile and occur along the diagonal bisector of the corner.

5. Westergaard's equations for determining the distance, along the diagonal bisector of the corner, from the corner to the maximum corner stress give values in close agreement with results obtained from the model tests.

6. Westergaard's equations for maximum corner stress along the diagonal bisector of the corner give values greater than corresponding stresses as measured in the model. (Westergaard's equations for maximum edge stresses are, as demonstrated earlier, in substantial agreement with corresponding stresses measured in the model.)

7. Critical stresses in a rigid pavement result from edge loading, the maximum corner stress being only 45 to 55 percent of the maximum edge stress.

REFERENCES

1. SPANGLER, M. G., "Stresses in the Corner Region of Concrete Pavements," Iowa Engineering Experiment Station Bulletin 157, 1942.
2. TELLER, L. W. AND SUTHERLAND, E. C., "The Structural Design of Concrete Pavements—Part V," Public Roads, April 1943.
3. KELLEY, E. F., "Application of the Results of Research to the Structural Design of Concrete Pavements," Public Roads, July and August 1939.
4. MELLINGER, F. M. AND CARLTON, P. F., "Application of Models to Design Studies of Concrete Airfield Pavements," Proceedings Highway Research Board, Vol. 34, 1955.
5. WESTERGAARD, H. M., "New Formulas for Stresses in Concrete Pavements of Airfields," Transactions, American Society of Civil Engineers, Vol. 113, 1947.
6. WESTERGAARD, H. M., "Stresses in Concrete Pavements Computed by Theoretical Analysis," Public Roads, April 1926.
7. TIMOSHENKO, S., Theory of Elasticity. 1934, p. 33. McGraw-Hill, New York, N. Y.